Theory of Transient Permeation Through Reactive Barrier Films II. Two Layer Reactive-passive Structures with Dynamic Interface

Stanislav E. Solovyov [a] & Anatoliy Ya. Goldman [a]

[a] Department of Materials and Processing , Alcoa Closure Systems International, Inc. , Crawfordsville, Indiana, USA
Published online: 01 Sep 2006.

PLEASE SCROLL DOWN FOR ARTICLE

primary sources of information. Taylor and Francis shall not be liable for any losses, actions, claims, proceedings, demands, costs, expenses, damages, and other liabilities whatsoever or howsoever caused arising directly or indirectly in connection with, in relation to or arising out of the use of the Content.

This article may be used for research, teaching, and private study purposes. Any substantial or systematic reproduction, redistribution, reselling, loan, sub-licensing, systematic supply, or distribution in any form to anyone is expressly forbidden. Terms & Conditions of access and use can be found at http://www.tandfonline.com/page/terms-and-conditions

Taylor & Francis
Taylor & Francis Group

THEORY OF TRANSIENT PERMEATION THROUGH REACTIVE BARRIER FILMS II. TWO LAYER REACTIVE-PASSIVE STRUCTURES WITH DYNAMIC INTERFACE

Stanislav E. Solovyov
Anatoliy Ya. Goldman
Department of Materials and Processing, Alcoa Closure Systems
International, Inc., Crawfordsville, Indiana, USA

The theory of transient permeation through homogeneous and structures incorporating non−catalytic solute scavenger is developed in Part II. It is based on the authors' earlier analytical solutions for the steady state model of permeation through passive films and reactive films with immobile catalytic scavenger dispersed within the layer. For consumable scavengers, the steady-unsteady solution matching method is introduced to describe scavenger consumption dynamics as a moving interface between reactive and passive layers of the film. The scavenger exhaustion time equation is derived in the approximation of fast reaction but it is shown to be also valid for intermediate reaction rates. The transient transmission rate dependence on time, boundary conditions, reactivity and reactive capacity of the scavenger, and layer sequence is derived. The terminology, notation, and section numbering continue from Part I of this series [1].

9. TWO PASSIVE LAYER LAMINATE (PP-FILM)

For completeness of the discussion of multilayer reactive structures the known solution for two-layer passive-passive barrier film is reproduced. The first layer (exposed to external partial pressure p_{in} of the permeant inside the package) has thickness L_1, diffusivity D_1, solubility S_1, and the

second layer has the respective L_2, D_2, S_2. In steady state the fluxes J_1 and J_2 through both layers are the same, and the linear solution (Eq. 6.2) for Eq. 6.1 described in Part I [1] holds for each respective layer. Thus, using the expression in Eq. 6.3 for the flux we obtain

$$J_x = J_0 = -\frac{D_1}{L_1}(C_1 - C_{in}) = -\frac{D_2}{L_2}(C_{out} - C_2) \qquad (9.1)$$

where C_1 and C_2 are solute concentrations on the respective sides of layer 1 and layer 2 interface. Assuming instant equilibrium of the solute at the interface partial pressures of the solute on both sides of the interface are equal: $p_1 = p_2$ can be written using Henry's law:

$$\frac{C_1}{S_1} = \frac{C_2}{S_2} \qquad (9.2)$$

Solving system Eqs. 9.1 and 9.2 for C_1 and C_2 we get

$$C_1 = \frac{1}{S_2} \cdot \frac{\frac{L_1}{D_1}C_{out} + \frac{L_2}{D_2}C_{in}}{\frac{L_1}{D_1 S_1} + \frac{L_2}{D_2 S_2}} \qquad (9.3)$$

$$C_2 = \frac{S_2}{S_1}C_1 \qquad (9.4)$$

and finally for the flux J_0:

$$J_0 = J_x = -\frac{\frac{C_{out}}{S_2} - \frac{C_{in}}{S_1}}{\frac{L_1}{D_1 S_1} + \frac{L_2}{D_2 S_2}} = \frac{-\Delta p}{\frac{1}{TR_1} + \frac{1}{TR_2}} \qquad (9.5)$$

The well-known result easily follows from Eq. 9.5 after applying the definition in Eq. 4.5 for the effective transmission rate TR_{eff}

$$TR_{eff} = \frac{1}{\frac{1}{TR_1} + \frac{1}{TR_2}} \qquad (9.6)$$

This result can be routinely expanded to multilayer films with any number of consecutive passive layers [2−3]:

$$TR_{eff} = \frac{1}{\frac{1}{TR_1} + \frac{1}{TR_2} + \cdots + \frac{1}{TR_N}} \qquad (9.7)$$

although for a heterogeneous structure only the transmission rate TR_{eff} rather than the often reported effective permeability P_{eff} has physical
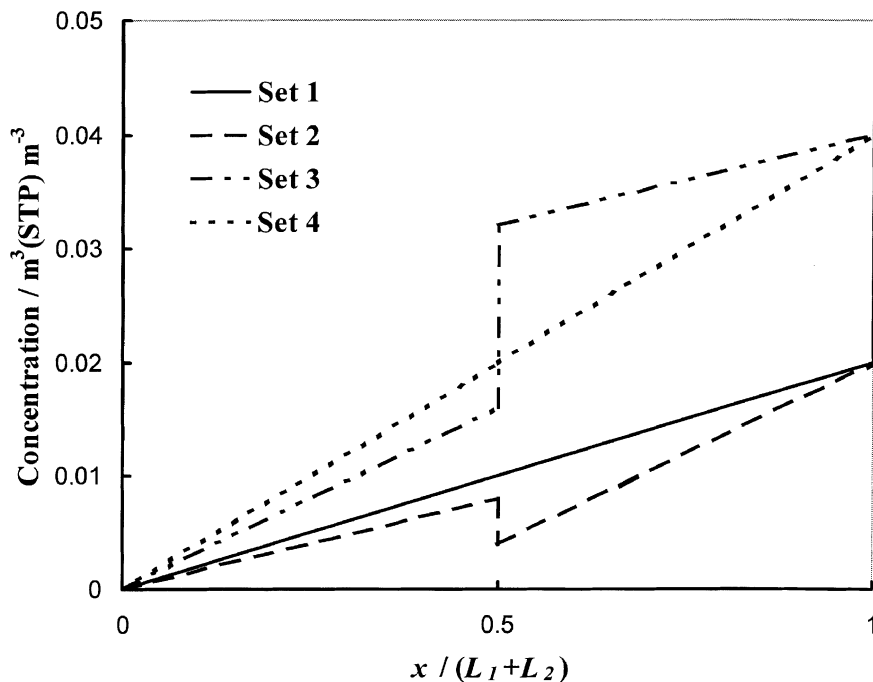
FIGURE 1 Solute concentration profiles in PP-film. $C_{in} = 0$.

meaning [3] and should be used in Eq. 9.7 instead of the ratio P_{eff}/L_{total}:

$$TR_{eff} = \frac{1}{\frac{L_1}{P_1} + \frac{L_2}{P_2} + \cdots + \frac{L_N}{P_N}} \tag{9.8}$$

It is noted that for passive barriers the effective transmission rate does not depend on the sequence of layers, and the solute flux is the same across any plane $x = $ const. Figure 1 presents some typical steady state solute concentration profiles for 4 sets of PP-films described in Table 1.

TABLE 1 Dimensionless Parameter Settings for Figures 1–3. All Materials Properties are Normalized to Scaling Set (5.1). $L_1 = L_2 = 1$

	D_1	S_1	D_2	S_2
Set 1	1	1	1	1
Set 2	2	2	1	1
Set 3	1	1	2	2
Set 4	1	2	1	2

10. TWO-LAYER FILM WITH THE REACTIVE LAYER EXPOSED TO THE PACKAGE CONTENTS (RP-FILM)

Let's consider a two-layer film where the first layer (exposed to p_{in}) is reactive (R) with corresponding thickness L_1, diffusivity D_1, solubility S_1, and reaction rate constant k_1, and the second layer is passive (P) with L_2, D_2, S_2 (see Figure 2). Such a structure can be called an *RP-film*. In this case there are four unknown parameters: C_1 and C_2 for interfacial solute concentrations and coefficients β_1, β_2 for the reactive layer. C_1 and C_2 denote steady state solute concentrations at the reactive (1) and passive (2) side of the interface between two layers. Using the solution in Eq. 3.2 for the reactive layer the relations on the reaction layer boundaries can be written as:

$$C_{in} = \beta_1 + \beta_2 \tag{10.1}$$

$$C_1 = \beta_1 \exp(\phi_1) + \beta_2 \exp(-\phi_1) \tag{10.2}$$

Here, ϕ_1 is Thiele modulus for the reactive layer:
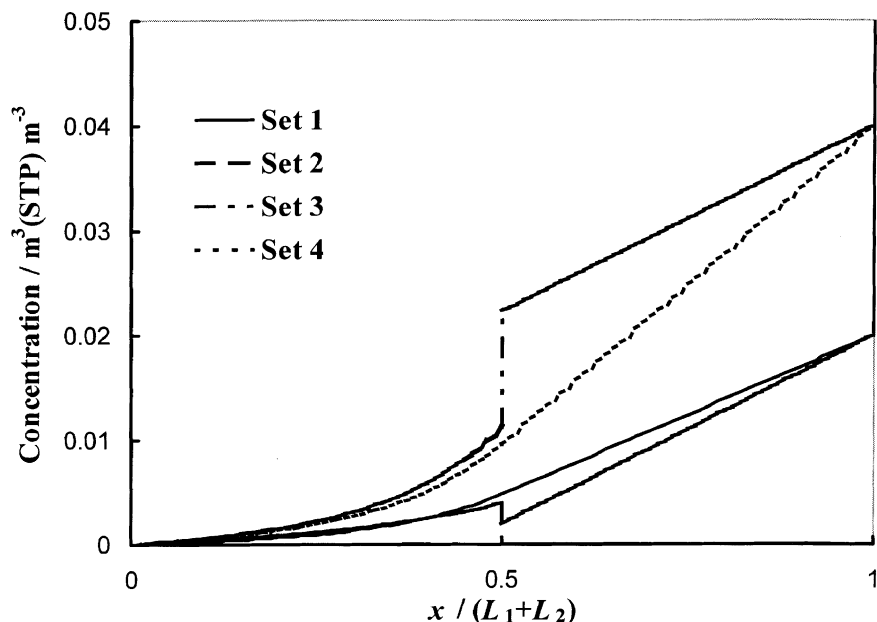
$$\phi_1 = L_1 \sqrt{\frac{k_1}{D_1}} \tag{10.3}$$

FIGURE 2 Solute concentration profiles in RP-film. $C_{in} = 0$, $R = $ const.

It is assumed that there is an established steady state at the reactive-passive layer interface; then the partial pressures of the permeant on both sides of the interface have to be the same:

$$p_1 = p_2 \tag{10.4}$$

Utilizing Henry's law on both sides of the interface as in Eq. 9.2, we find from Eq. 10.4:

$$\frac{C_1}{S_1} = \frac{C_2}{S_2} \tag{10.5}$$

In addition to Eqs. 10.1, 10.2, and 10.5 one more relation between four unknowns to close the system are needed. It follows from the observation that the solute flux across the interface should be the same on both sides of the interface to avoid accumulation or depletion of the solute within the interface. Equaling Eq. 6.3 for flux through passive barrier and Eq. 7.3 for the flux through active barrier at $x = L_1(\xi = 1$ for the reactive layer), we write

$$\frac{D_2}{L_2}(C_{out} - C_2) = \sqrt{k_1 D_1}(\beta_1 \exp(\phi_1) - \beta_2 \exp(-\phi_1)) \tag{10.6}$$

Eqs. 10.1, 2, 5, 6 form a system of linear equations with 4 unknowns. For convenience they are rewritten in matrix form:

$$\begin{bmatrix} 0 & 0 & 1 & 1 \\ 1 & 0 & -c_1 & -1/c_1 \\ 1 & -d & 0 & 0 \\ 0 & 1 & c_1 e_1 f_2 & -e_1 f_2/c_1 \end{bmatrix} \times \begin{bmatrix} C_1 \\ C_2 \\ \beta_1 \\ \beta_2 \end{bmatrix} = \begin{bmatrix} a \\ 0 \\ 0 \\ b \end{bmatrix} \tag{10.7}$$

where the known parameters are defined as follows:

$$\begin{aligned} a &= C_{in} \\ b &= C_{out} \\ c_1 &= \exp(\phi_1) \\ d &= \frac{S_1}{S_2} \\ e_1 &= \sqrt{k_1 D_1} \\ f_2 &= \frac{L_2}{D_2} \end{aligned} \tag{10.8}$$

The unique solution of the system in Eq. 10.7 can be found provided the system is non-degenerate or its determinant δ is not equal to zero. That condition has a form:

$$\delta_1 = (c_1^2 + 1)(de_1 f_2 + 1) - 2 \neq 0 \tag{10.9}$$

When the condition $\delta_1 \neq 0$ is satisfied, the analytical solution of Eq. 10.7 is obtained as

$$C_1 = \frac{d}{\delta_1}(2ac_1 e_1 f_2 + b(c_1^2 - 1))$$

$$C_2 = \frac{1}{\delta_1}(2ac_1 e_1 f_2 + b(c_1^2 - 1))$$

$$\beta_1 = \frac{1}{\delta_1}(a(de_1 f_2 - 1) + bc_1 d) \tag{10.10}$$

$$\beta_2 = \frac{1}{\delta_1}(ac_1^2(de_1 f_2 + 1) - bc_1 d)$$

The effective flux J_0 through the RP film is found using Eq. 7.4 for the reactive layer:

$$J_0 = -\sqrt{k_1 D_1}(\beta_1 - \beta_2) = \frac{-e_1}{\delta_1}(a[(1 - c_1^2)de_1 f_2 - (1 + c_1^2)] + 2bc_1 d) \tag{10.11}$$

Figure 2 demonstrates typical solute concentration profiles in RP films with $k_1 = 10$ and $L_1 = L_2 = 1$ normalized according to Eq. 5.1 and corresponding to Thiele modulus $\phi_1 = 3.16$.

11. TWO-LAYER FILM WITH THE REACTIVE LAYER EXPOSED TO THE ENVIRONMENT (PR-FILM)

Let's consider a PR-film where the first layer (exposed to p_{in}) is passive (P) with parameters L_1, D_1, S_1, and the second layer is reactive (R) with L_2, D_2, S_2, k_2 as shown in Figure 3. Utilizing the same procedure as in the preceding section, we end up with the following system of equations:

$$C_2 = \beta_1 + \beta_2 \tag{11.1}$$
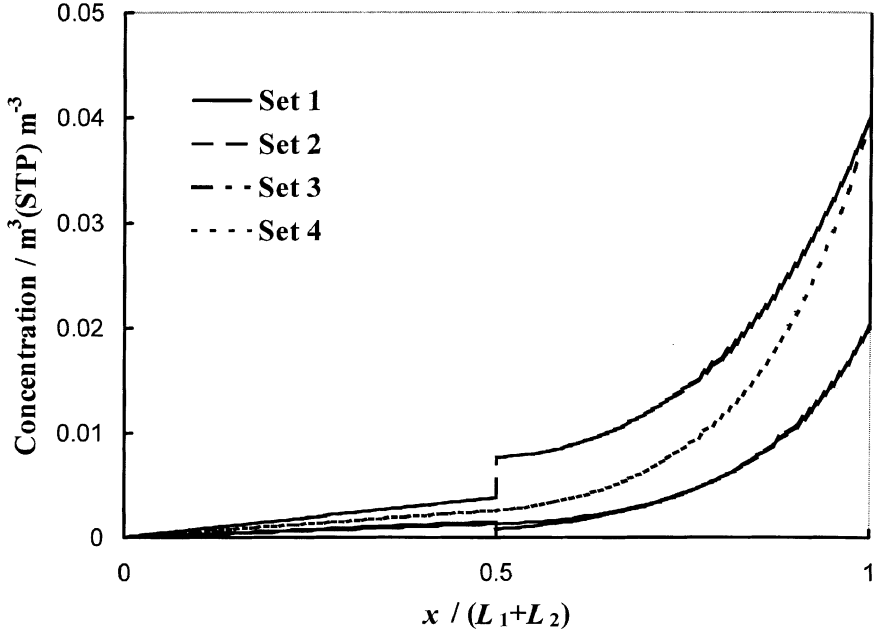
FIGURE 3 Solute concentration profiles in PR-film. $C_{in} = 0$, $R = \text{const.}$

$$C_{out} = \beta_1 \exp(\phi_2) + \beta_2 \exp(-\phi_2) \tag{11.2}$$

$$\frac{C_1}{S_1} = \frac{C_2}{S_2} \tag{11.3}$$

$$\frac{D_1}{L_1}(C_1 - C_{in}) = \sqrt{k_2 D_2}(\beta_1 - \beta_2) \tag{11.4}$$

Here, ϕ_2 is Hatta number for the second (reactive) layer:

$$\phi_2 = L_2\sqrt{\frac{k_2}{D_2}} \tag{11.5}$$

In matrix form we get

$$\begin{bmatrix} 0 & -1 & 1 & 1 \\ 0 & 0 & c_2 & 1/c_2 \\ 1 & -d & 0 & 0 \\ 1 & 0 & -e_2 f_1 & e_2 f_1 \end{bmatrix} \times \begin{bmatrix} C_1 \\ C_2 \\ \beta_1 \\ \beta_2 \end{bmatrix} = \begin{bmatrix} 0 \\ b \\ 0 \\ a \end{bmatrix} \tag{11.6}$$

where the known parameters are defined as

$$
\begin{aligned}
a &= C_{in} \\
b &= C_{out} \\
c_2 &= \exp(\phi_2) \\
d &= \frac{S_1}{S_2} \\
e_2 &= \sqrt{k_2 D_2} \\
f_1 &= \frac{L_1}{D_1}
\end{aligned}
\tag{11.7}
$$

Non-degeneration condition for the system in Eq. 11.6 is

$$
\delta_2 = 2d - (1 + c_2^2)(d + e_2 f_1) \neq 0
\tag{11.8}
$$

Provided the condition $\delta_2 \neq 0$ is met, the unique solution of the system in Eq. 11.6 is

$$
\begin{aligned}
C_1 &= \frac{d}{\delta_2}(a(1 - c_2^2) - 2bc_2 e_2 f_1) \\
C_2 &= \frac{1}{\delta_2}(a(1 - c_2^2) - 2bc_2 e_2 f_1) \\
\beta_1 &= \frac{1}{\delta_2}(a - bc_2(d + e_2 f_1)) \\
\beta_2 &= \frac{1}{\delta_2}(-ac_2^2 + bc_2(d - e_2 f_1))
\end{aligned}
\tag{11.9}
$$

The effective flux J_0 through the PR-film can be found using Eq. 7.4 for the reactive layer, or Eq. 6.3 for the passive layer, because in PR-film the flux at the exit of the reactive layer is equal to the flux anywhere within the subsequent passive layers:

$$
J_0 = -\sqrt{k_2 D_2}(\beta_1 - \beta_2) = -\frac{e_2}{\delta_2}(a(1 + c_2^2) - 2bc_2 d)
\tag{11.10}
$$

Figure 3 demonstrates typical solute concentration profiles in PR-films with $k_2 = 10$ and $L_1 = L_2 = 1$ normalized according to Eq. 5.1 with $\phi_2 = 3.16$.

12. SIMPLIFIED WAVEFRONT SOLUTION FOR SCAVENGER CONSUMPTION

The steady state solutions for a reaction-diffusion system (Eqs. 2.1 and 2.2) were analyzed, assuming the scavenger is not consumed by the

reaction. That is not the case in actual applications; moreover, Eq. 2.2 suggests that when there is a solute concentration gradient within the reactive layer, the scavenger consumption rate will be higher where the permeant concentration is higher. Assuming some pseudo steady state concentration profile $C^*(x)$ in the reactive layer at a particular time moment $t = t^*$ and integrating Eq. 2.2 by t obtains an instantaneous snapshot of scavenger concentration profile around time t^* for fast reaction:

$$R(x, t^*) = R_0 \exp(-KC^*(x)t^*) \tag{12.1}$$

where $R_0 = R(x, 0) = \text{const}$ is the initial concentration of active sites. This attempt at decoupling the system of Eqs. 2.1 and 2.2 does not provide true solution because there is no steady state permeant concentration profile at any time when the scavenger is consumed by the reaction. However, it gives an idea how the scavenger concentration profile would evolve in the presence of solute concentration gradients. Figure 4 exemplifies the idea for several solute concentration profiles $C^*(x)$ from cases analyzed in Part I. Scavenger concentration profiles in Figure 4 are shown for the initial Thiele modulus ϕ_0 of the reactive layer and time t^* pairs (ϕ_0, t^*) with two different times selected to illustrate scavenger consumption dynamics. It is observed that for intermediate values of ϕ_0 there is no well-defined reaction wavefront and the steady state is reached faster than for large ϕ_0 when the reaction
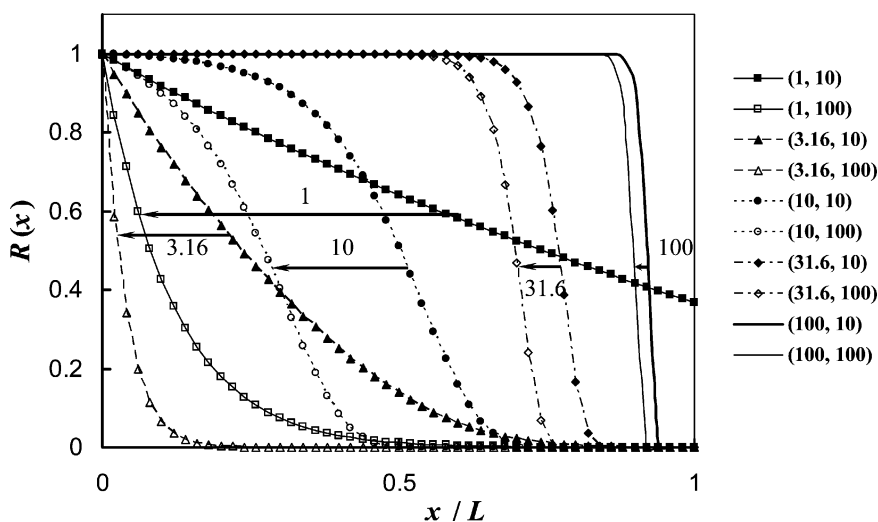

FIGURE 4 Scavenger concentration profiles in R-film. $C_{in} = 0$, $R \neq \text{const}$.

wavefront is narrow and moves slowly. Intermediate ϕ_0 values of the order of 1 correspond to the joint activation and diffusion control of the overall reaction rate and are of the most practical interest. For $\phi_0 \ll 1$ diffusion dominates and the overall reaction rate is activation controlled. For $\phi_0 \gg 1$ the reaction is fast and the overall reaction rate is diffusion controlled. The effect of the fast reaction depends on whether the reaction is catalytic or non-catalytic. The catalytic reaction does not consume the scavenger and quickly leads to establishment of the steady state permeation pattern characterized by very small effective flux exiting the membrane. The non-catalytic reaction triggers transient permeation process of heterogeneous scavenger capacity consumption that can be extremely long.

It is noted that when the reaction is fast ($\phi_0 \gg 1$) and the reaction zone is narrow, an approximate analytical solution for the exhaustion lag time was derived by Yang et al. [4] in terms of slowly moving reaction wavefront, which effectively reduces the thickness of the layer with active scavenger as it propagates consuming all available scavenger and stoichiometric amount of the solute. All the reaction takes place within the wavefront, but no reaction occurs before and after it, thus a delta-function is assumed to be a solution for the scavenger concentration at any time moment. The unsteady state mass balance for the scavenger within the slowly moving front can be written then as

$$\frac{d}{dt}(AL_d^* R_0) = \frac{AJ_f}{\mu} \qquad (12.2)$$

where J_f is the positive permeant flux into the front, A is the barrier area, $\mu = C/R$ is the scavenger reactive capacity defined as the stoichiometric coefficient for the amount of the permeating species consumed by the amount of the scavenger active sites in unit polymer volume expressed in $[\text{m}^3 \, (\text{STP}) \, \text{mol}^{-1}]$, and $L_d^* = L_d^*(t)$ is the front position moving downstream relative to the outer film boundary $x = L$ recorded along the coordinate

$$x^* = L - x \qquad (12.3)$$

with the initial condition

$$\text{at } x^* = 0\text{: } L_d^*(0) = 0 \qquad (12.4)$$

Assuming $C_{in} = 0$ and exact stoichiometry in the front (meaning all the solute reaching the front is consumed by the scavenger: $C_f = C(L_d(t), t) = 0$), Yang et al. obtained the following expression for the flux J_f in x^* coordinates:

$$J_f = -D\frac{dC}{dx^*}\bigg|_{x^*=L_d^*} = \frac{-D}{L_d^*}(C_f - C_{out}) = \frac{DC_{out}}{L_d^*} \tag{12.5}$$

Combining Eqs. 12.2, 12.4, and 12.5 reproduces Yang et al.'s result:

$$L_d^*(t) = \sqrt{\frac{2DC_{out}t}{\mu R_0}} \tag{12.6}$$

Then in the original coordinate system x the front position $L_d(t)$ is given by

$$L_d(t) = L - \sqrt{\frac{2DC_{out}t}{\mu R_0}} \tag{12.7}$$

It is noted that this concept for estimating the reaction front velocity for fast reaction can also be applied in the case $C_{in} > 0$: then it would require the introduction of the opposite wavefront propagating upstream from the inner boundary $x = 0$:

$$L_u(t) = \sqrt{\frac{2DC_{in}t}{\mu R_0}} \tag{12.8}$$

if the initial condition $C(x,0) = 0$ for the solute free film is assumed.

13. REFERENCE LAG TIME

To analyze the reference lag time in a passive film ($K = 0$):

$$\frac{\partial C}{\partial t} = D\frac{\partial^2 C}{\partial x^2} \tag{13.1}$$

the authors used initial conditions different from those originally imposed in Eq. 2.9. In passive barriers the lag time refers to the intercept of the asymptotic steady state flux across the film with the time axis when initially the film is free of the permeating species. The initial conditions for the permeant are then

$$0 \leq x \leq L: \quad C(x,0) = 0 \tag{13.2}$$

$$x < 0: \quad p_{in}(x,0) = 0 \tag{13.3}$$

$$x > L: \quad p_{out}(x,0) = p_{out} \tag{13.4}$$

and boundary conditions for $t > 0$:

$$x = 0 \quad C(0,t) = 0 \tag{13.5}$$

$$x = L \quad C(L,t) = Sp_{out} \tag{13.6}$$

The reference lag time t_L is defined for passive barriers. For monolayer homogeneous material, the solution in terms of expansion series is well known (Daynes [5], Barrer [6]):

$$C(x,t) = C_{in} + (C_{out} - C_{in})\frac{x}{L}$$

$$+ \frac{2}{\pi}\sum_{n=1}^{\infty}\frac{C_{out}\cos n\pi - C_{in}}{n}\sin\frac{n\pi x}{L}\exp(-Dn^2\pi^2 t/L^2)$$

$$+ \frac{4C_0}{\pi}\sum_{m=0}^{\infty}\frac{1}{2m+1}\sin\frac{(2m+1)\pi x}{L}\exp(-D(2m+1)^2\pi^2 t/L^2) \tag{13.7}$$

then using Fick's first law (Eq. 4.1) we find the ingress I(t) as the total amount of the solute passed through the film in time t as $t \to \infty$:

$$I(t) = \frac{DC_{out}}{L}\left(t - \frac{L^2}{6D}\right) \tag{13.8}$$

with the intercept with the time axis given by

$$t_L = \frac{L^2}{6D} \tag{13.9}$$

We shall use the term *Daynes lag time* to denote this purely diffusive delay in establishing steady state permeation pattern after a sudden change in permeant pressure outside the film.

Siegel's result [5] for the reactive film with the catalytic scavenger $R(x, t) = $ const corresponding to $\phi = $ const, and $C_{in} = 0$, which reproduced an earlier result by Leypolt and Gough [7], demonstrated that the lag time to reach the asymptotic behavior is reduced as the reaction rate k increases:

$$t_L = \frac{L^2}{6D}\left(\frac{3(\phi\coth\phi - 1)}{\phi^2}\right) \tag{13.10}$$

That result (Eq. 13.9) is recovered from Eq. 13.10 for the passive barrier case when $k = 0$. The same result is expected for the consumable scavenger if the characteristic time of diffusion through the film is much shorter than time for a meaningful scavenger capacity reduction. In that case t_L characterizes the transition to reactive permeation rather than the asymptotic behaviour at $t \to \infty$.

14. EXHAUSTION LAG TIME

In the case of reactive film with fast reaction and $C_{in} = 0$, the exhaustion lag time t_{LE} during which the scavenger capacity is completely exhausted by the reaction with the permeant is found from Eq. 12.6 by setting $L_d^*(t_{LE}) = L$ as

$$t_{LE} = \frac{L^2}{2D} \frac{\mu R_0}{C_{out}} \tag{14.1}$$

For $C_{in} > 0$ and $C_0 = 0$, t_{LE} can be found as the time at which two opposite wave fronts (Eqs. 12.7 and 12.8) propagating from the opposite film boundaries collide:

$$L_d(t_{LE}) = L_u(t_{LE}) \tag{14.2}$$

Then the lag time to front collision is found as

$$t_{LE} = \frac{L^2}{2D} \cdot \frac{\mu R_0}{(C_{out} + C_{in} + 2\sqrt{C_{out}C_{in}})} \tag{14.3}$$

It is seen that for fast reaction the nonzero solute concentration C_{in} inside the package can significantly reduce the lifetime of the scavenger. Also, the lag time t_{LE} with consumable scavenger $R(x, t) \neq$ const in the considered simplified case does not depend on the reaction rate constant k (for $\phi_0 \gg 1$) but only on the film scavenging capacity μR_0 and the boundary conditions. On the other hand, the effective flux J_0 for such a system does depend on k at any position of the reaction wavefront as shown by the result in Eq. 10.11 for RP-films and as suggested by experimental data. The wavefront position in static RP-film terms is defined as the position of the reactive-passive layer interface at $x = L_1$. If the front is moving, then $L_1 = L_1(t)$ and $L_2 = L_2(t)$, but $L_1(t) + L_2(t) \equiv L = $ const. Note that in Eq. 10.11, the parameters $c_1 = \exp(\phi_1)$ and $f_2 = L_2/D_2$ explicitly depend on L_1 and L_2, respectively. Thus, there is a necessity to develop a generalized solution for propagating reaction wavefront and nonzero effective flux through the film during its propagation.

15. STEADY-UNSTEADY SOLUTION MATCHING FOR PARTIALLY PERMEABLE REACTION WAVEFRONT

Simplified solutions in Eqs. 14.1 and 14.3 were obtained assuming the permeant flux J_f that drives the wavefront is found according to Eq. 12.5, that is, that $C_f = 0$. That assumption results in zero effective flux exiting the membrane during t_{LE}, i.e., the scavenger exhaustion time t_E coincides with the *steady state* lag time t_L^{SS} and it is called the exhaustion lag time t_{LE}. The relationship between the steady state lag time t_L^{SS} (defined for the initial conditions of steady state flux across a passive membrane) and the reference lag time t_L will be discussed in Part III. Considering the permeant concentration profiles in Figure 2 it was observed that a more accurate solution may be obtained if $C_f = C_2$ is used according to the analytical solution in Eq. 10.10. Because $C_2 > 0$ for any wavefront position $L_d(t) > 0$, Eq. 12.5 leads to overestimating the scavenger exhaustion time also producing zero transient transmission rates not observed experimentally when reaction is not instantaneous ($\phi < \infty$). In fact, when $\phi < \infty$ it is easy to see from reaction kinetics equations that t_E should be infinite since the reaction with finite rate k will never completely exhaust the scavenger reactive capacity when $C_{in} = 0$. That statement is only true when concentration based reaction kinetic models are considered: in actual systems with localized non-catalytic scavenging sites, their capacity will be exhausted in a long but finite time. Considering that the asymptotics of reaching the steady state permeation may be slow but at longer times its effect on permeant ingress is negligible, a better description of transient permeation during times on the t_{LE} order of magnitude is sought.

To improve the solution in Eq. 14.1 the steady-unsteady solution matching (SUSM) method is introduced: if the reaction is fast so that the transient Thiele modulus for the reactive layer $L_d(t)$ with full scavenging capacity μ and reactivity k:

$$\phi_R(t) = L_d(t)\sqrt{\frac{k}{D}} \gg 1 \qquad (15.1)$$

then a narrow reaction wavefront propagating downstream by depleting the scavenger concentration can be assumed. Assuming that the wavefront moves slowly enough so that pseudo steady state of the solute concentration adjusting to its movement is achieved throughout the film, the approximate unsteady state mass balance (Eq. 12.2) for R on the front holds, and the solution in Eqs. 10.9 and 10.10 for the solute concentration in RP-film applies with the RP layer interface defining

the wavefront position $L_d(t)$. The net effect is that the narrow scavenger concentration wavefront becomes partially permeable to the solute, but the solute permeated ahead of the front does not consume the scavenger. This two zone approximation means splitting the continuous scavenger concentration profile into completely reacted layer behind the front and unreacted layer ahead of it where a small amount of permeating solute does not significantly affect the scavenger reactive capacity.

The feasibility of the partial permeability of the reaction front stems from the fact that the scavenger is usually a particulate that forms a physically separate phase from the polymer matrix, thus bulk reaction equations valid for gases do not provide an adequate description of the diffusing solute reaction with the dispersed scavenger. Some diffusing solute is bound to miss localized scavenging sites and penetrate beyond the narrow reaction zone even for very fast reactions. The exact fraction of the solute permeating through the reaction front is determined by the probability of solute molecule collision with the scavenger particle during solute residence time in the front and the activation energy of the reaction. That probability in turn depends on the scavenger volume fraction, dispersion of the scavenger (i.e., its average particle size for the specific load), diffusivity of the matrix and local permeant flux into the front. When the scavenger particle size approaches the characteristic molecular dimensions of the matrix polymer and the system approaches homogeneity, it is expected for the solute fraction permeating through the reaction wavefront to be in agreement with the catalytic reaction solution (7.4) for the effective flux which exponentially goes to zero as Thiele modulus of the reactive layer is increased.

Observing that the amount of the solute C penetrating through the reaction front into the unreacted layer is small, it can be postulated that the solute consumption rate μKRC with the scavenger is negligible: $\mu KRC \approx 0$ for $x < L_d(t)$, and it does not significantly affect the scavenger concentration R ahead of the front. Then there is justification to match the steady state solution in Eqs. 10.9 and 10.10 for renewable scavenger with the impermeable wavefront Eq. (12.2). Substituting C_2 from Eq. 10.10 into Eq. 12.5 we find the flux J_f into the front as

$$J_f = -D\frac{dC}{dx^*}\bigg|_{x^*=L_d^*} = \frac{D(C_{out} - C_2)}{L_d^*} = \frac{DC_{out}}{L_d^*} \cdot \frac{(c_1^2 + 1)e_1 f_2}{(c_1^2 + 1)e_1 f_2 + (c_1^2 - 1)} \tag{15.2}$$

Assuming that permeant diffusivity D and solubility S in the film before and after the scavenging reaction are unchanged: $D = D_1 = D_2$,

$S = S_1 = S_2$, that $k \equiv k_1$ is the only reaction rate constant in the system, and keeping in mind the matching definitions

$$L_1 = L_d(t) = L - L_d^*(t) \tag{15.3}$$

$$L_2 = L - L_d(t) = L_d^*(t) \tag{15.4}$$

the two parameter complexes present in Eq. 15.2 can be defined as

$$Z \equiv e_1 f_2 = \sqrt{k_1 D_1} \cdot \frac{L_2}{D_2} = L_2 \sqrt{\frac{k}{D}} = L_d^*(t)\sqrt{\frac{k}{D}} \tag{15.5}$$

$$Y \equiv c_1^2 = \exp\left(2L_1\sqrt{\frac{k_1}{D_1}}\right) = \exp\left(2(L - L_d^*(t))\sqrt{\frac{k}{D}}\right) = \exp(2(\phi_0 - Z)) \tag{15.6}$$

Here $\phi_0 = \phi_R(0)$ is the initial Thiele modulus, which is a constant for any particular reactive layer and scavenger load. Comparing the relation of Eq. 15.5 to Eq. 15.1 it is noted that complex Z may be called *reciprocal Thiele modulus* for the RP-film because it exhibits the synergetic effect of reaction in the active layer and diffusion in the passive layer as the wavefront propagates. Using the definitions in Eqs. 15.5 and 15.6, Eq. 15.2 may be rewritten as

$$J_f = C_{out}\sqrt{kD} \cdot \frac{\exp(2(\phi_0 - Z)) + 1}{(\exp(2(\phi_0 - Z)) + 1) \cdot Z + \exp(2(\phi_0 - Z)) - 1} \tag{15.7}$$

From Eq. 12.2 can be obtained

$$\frac{dL_d^*(t)}{dt} = \frac{J_f}{\mu R_0} \tag{15.8}$$

and then rewriting Eq. 15.8 using Eq. 15.5 and 15.7:

$$\frac{dZ}{dt} = \frac{kC_{out}}{\mu R_0} \cdot \frac{(\exp(2(\phi_0 - Z)) + 1)}{(\exp(2(\phi_0 - Z)) + 1) \cdot Z + \exp(2(\phi_0 - Z)) - 1} \tag{15.9}$$

After taking into account the initial condition $L_d^*(0) = 0$, that is, $Z = 0$ at $t = 0$, and using the definition in Eq. 15.3 and Eq. 15.6 to write

$$L_d(t) \equiv (\phi_0 - Z)\sqrt{\frac{D}{k}} \tag{15.10}$$

we find the analytical integral of Eq. 15.9 as

$$t = \frac{\mu R_0}{k C_{out}} \left[\frac{Z^2}{2} - Z + \ln\left(\frac{1 + e^{2\phi_0}}{1 + e^{2(\phi_0 - Z)}} \right) \right]$$

$$= \frac{\mu R_0}{C_{out}} \left[\frac{(L - L_d)^2}{2D} - \frac{L - L_d}{\sqrt{kD}} + \frac{1}{k} \ln\left(\frac{1 + \exp(2L\sqrt{k/D})}{1 + \exp(2L_d\sqrt{k/D})} \right) \right] \quad (15.11)$$

representing the time for the wavefront to reach the position L_d corresponding to a particular value of Z. The value of the approximate solution, thereafter called the Solovyov-Goldman (SG) model represented by Eqs. 10.9−11 and 15.11, is not only in predicting the scavenger exhaustion times but also in describing the dynamics of wavefront propagation and the corresponding transient transmission rates through the reactive film. It is noted that Eq. 15.11 is reduced to the Yang-Nuxoll-Cussler (YNC) model (Eq. 12.7) when $k \to \infty$. As Figure 5 demonstrates, the SG model provides a physically meaningful approximate solution $L_d(t)$ for the entire range of $t = [\phi \ldots t_E^+]$. Here t_E^+ is the scavenger capacity exhaustion time predicted by the SG model. The results shown in Figure 5 correspond to a base case (Eq. 5.1) with the respective k normalization. That makes the SG
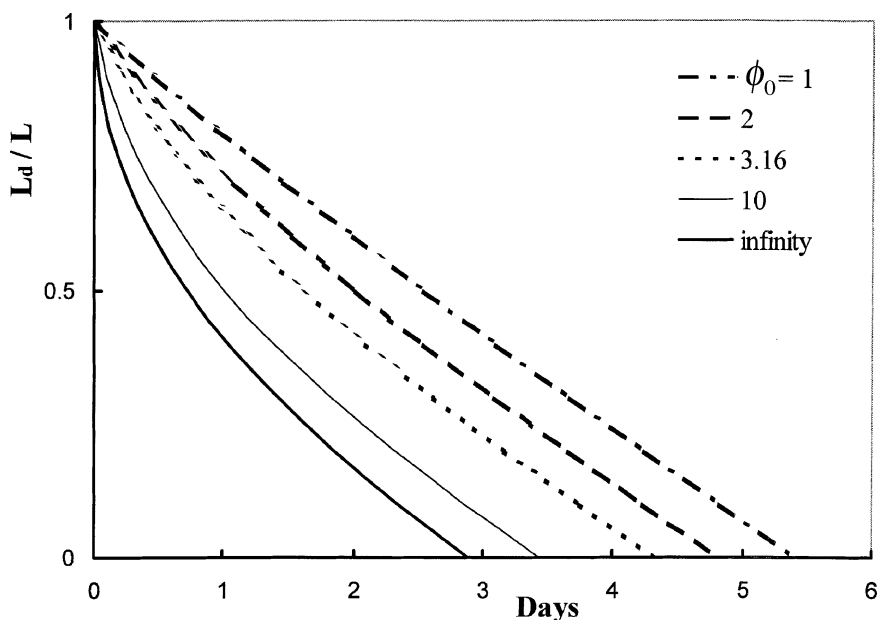

FIGURE 5 Reaction wavefront position versus time predicted by SG model.

model more attractive for the intermediate initial Ha values than the YNC model, which is stated to be valid only for $Ha > 100$.

To summarize, the SUSM method allows us to overcome the earlier unrealistic assumption that the moving reaction wavefront does not allow any solute permeation through it, or in other words, that exact stoichiometry of the solute consumed by the present amount of scavenger is maintained in the front. The YNC simplified solution assumed that the front movement is driven by complete scavenger exhaustion in the reactive plane exposed to solute flux, and any solute penetration beyond the front constitutes the front movement. The authors utilize the partially permeable propagating wavefront concept to estimate exhaustion times. However, the steady state solution defined by Eqs. 10.9–10 and instantly adjusting to slowly moving front is used to calculate the effective flux through the film according to Eq. 10.11. Thus, the SUSM method allows us to relax the exact stoichiometry assumption in the front and to predict nonzero solute concentrations ahead of the reactive zone by matching Eq. 6.2 and 3.2 with match conditions (Eq. 10.9–10) providing a more realistic physical description of the transient permeation process.

16. SCAVENGER EXHAUSTION TIME

The SG model provides a more accurate prediction of the wavefront position versus time for intermediate values of k (in terms of initial Thiele modulus ϕ_0. It is noted that the result in Eq. 15.11 does depend on the reaction rate k, and also the result in Eq. 12.6 is recovered from Eq. 15.11 for instantaneous reactions with $k = \infty$.

The scavenger exhaustion time t_E^+ is found from Eq. 15.11 by setting $Z(t_E^+) = \phi_0$, that is, $L_d(t_{LE}^+) = 0$:

$$t_E^+ = \frac{\mu R_0}{C_{out}}\left[\frac{L^2}{2D} - \frac{L}{\sqrt{kD}} + \frac{1}{k}\ln\left(\frac{1 + \exp(2L\sqrt{k/D})}{2}\right)\right]$$
$$= \frac{\mu R_0}{kC_{out}}\left[\frac{\phi_0^2}{2} - \phi_0 + \ln\left(\frac{1 + e^{2\phi_0}}{2}\right)\right]$$

Figure 6 demonstrates the relationship between the SG model approximation of the steady state lag time t_L^+, exhaustion time t_E^+ and exhaustion lag time t_{LE} in terms of downstream concentration growth dynamics for the scavenging reaction rates varying from zero to infinity. Figure 7 presents the comparison of earlier results in Eqs. 13.9, 13.10, and 14.1 and the solution in Eq. 16.1 for the exhaustion time (note that the exhaustion lag time refers to the time of
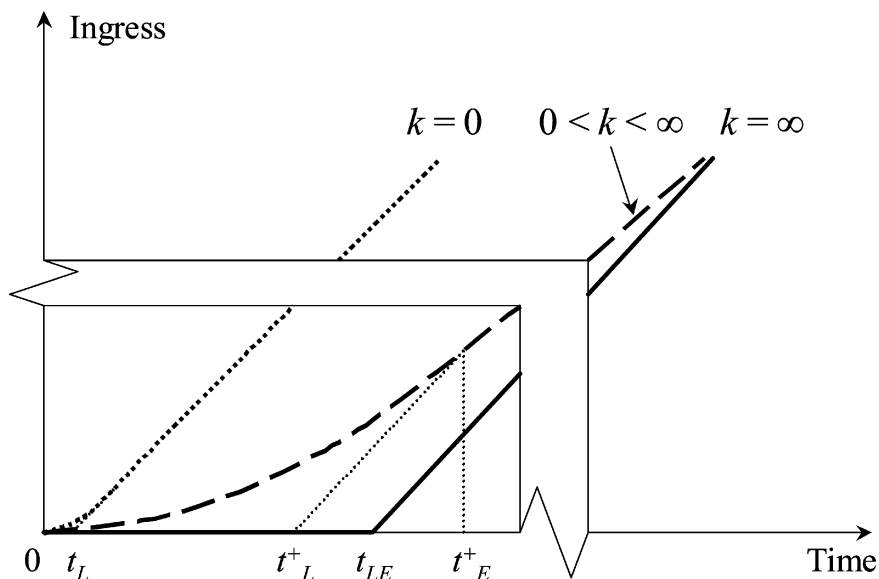
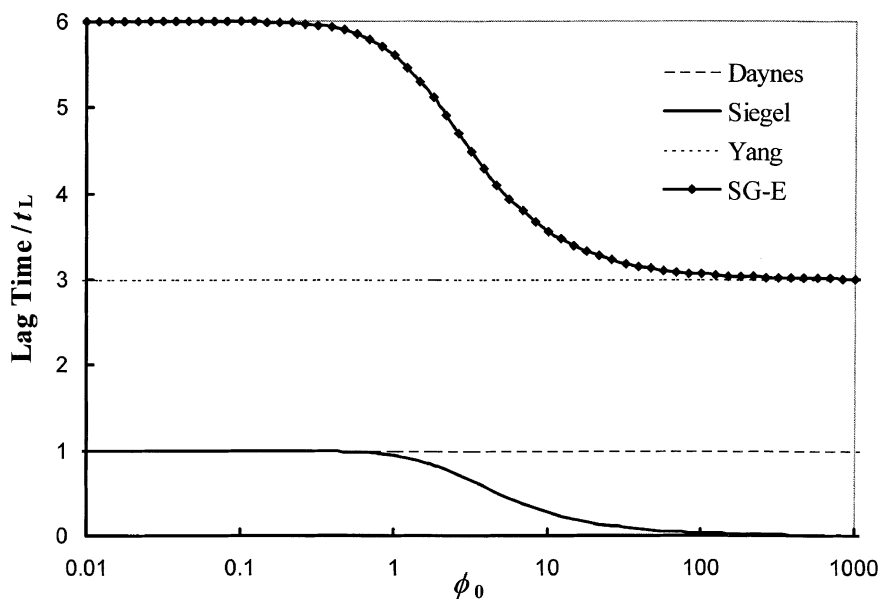**FIGURE 6** Relationship between scavenger exhaustion and reference lag times.

FIGURE 7 Lag time dependence on Thiele modulus ϕ (Siegel), ϕ_0 (Yang and SG models). Scavenger exhaustion time t_E is shown for SG model.

complete depletion of the scavenger reactive capacity: the steady state lag time t_L^+ for R-film, defined in line with the reference lag time t_L for P-film as the time axis intercept with asymptote of the solute concentration growth downstream, would be smaller than both t_E^+ and t_{LE} for $k < \infty$. This is a subject of the authors further work on optimal design of reactive-passive membranes). The x-axis dimensionless variable ϕ_0 is used in Figure 7 for convenience to represent variation in the rate constant k only, whereas parameters L and D are kept constant. All lag times are normalized to Daynes' lag time for P-film. The value of YNC lag time is determined by the dimensionless reactive scavenging capacity of the film material.

$$\Psi = \frac{\mu R_0}{C_{out}} \tag{16.2}$$

which was set at $\Psi = 1$ in Figure 7 for presentation clarity, resulting in $t_{LE} = 3t_L$ according to Eqs. 13.9 and 16.1, but it can be a very large number for novel scavenging systems. For example, for the R-film with all normalized properties equal to 1 and under permeant pressure gradient of 0.2 atmospheres the value $\Psi = 50$ is obtained.

It is noted that Siegel's solution exhibits a pattern of dependence on ϕ_0 that is fundamentally different from YNC and SG solutions. Of course, Daynes' solution with no reaction corresponds to a single point at $\phi_0 = 0$, but it is represented in Figure 7 by a line for the clarity of discussion. Similarly, the YNC solution is valid only at $\phi_0 \to \infty$, and it represents the lower limit of the *exhaustion time*, which coincides with the steady state lag time for $\phi_0 = \infty$. Daynes' solution t_L for P-film and Siegel's solution for R-film with unlimited scavenging capacity $\mu = \infty$ represent the lag time during which the steady state flux across the film is asymptotically established. These solutions converge to t_L at $\phi_0 \to 0$ as expected, while at large values of ϕ_0 the reference lag time $t_L \to 0$. Thus, the reaction with a scavenger of unlimited capacity accelerates the time to reach the steady state, which itself is characterized by a very low effective flux at the downstream boundary when ϕ_0 is large. That flux is found according to Eq. 7.4 for R-film. With the consumable scavenger there is no steady state flux across the film until the scavenger capacity is completely exhausted, whereas scavenger depletion is a kinetic process of a different nature compared to pure diffusive transport in the initially solute−free membrane to asymptotically reach the steady state. Because of that, the YNC solution, based on the narrow reaction wavefront assumption valid for large ϕ_0, should not and does not converge to that of Daynes at zero ϕ_0 (compare to the modification of Eq. 14.1 suggested by Cussler and Yang [8]).

Note that the scavenger exhaustion time $t_E^+ = 2t_{LE}$ at $\phi_0 \to 0$: this is an artifact of the SUSM method replacing the infinite t_E by a finite value t_E^+. The SG solution obtained by using the SUSM method aims to approximate the gap between the two solutions ($\phi_0 = 0$ and $\phi_0 = \infty$) by truncating the (infinite) time at which the asymptotic system behavior is established. That approximation effectively widens the reaction zone for the solute concentration C while keeping the infinitely narrow (delta-function) reaction zone approximation for the scavenger concentration R. The resulting approximation of the steady state lag time t_L^+ based on SG model for t_E^+ is derived in Part III of the series.

Figure 8 demonstrates typical dynamics of the permeance in terms of effective flux $J_0(t)$, obtained from the result in Eq. 10.11 for RP-films using t_E^+ solution (Eq. 16.1) obtained by steady-unsteady solution matching method when $C_{in} = 0$. For comparison, experimental data for the transient transmission rate through the structurally identical reactive films with arbitrary (unquantified) reactivities are presented in Figure 9 to show the qualitative agreement of the authors' theoretical predictions with the experiment. The time $t = 0$ in Figure 9 was selected as a time at which the scavenger was fully activated within the reactive layer because the activation mechanism was not considered in either of the presented models (activation dynamics is shown for 3 experiments as the permeance at $t < 0$). It is observed that the
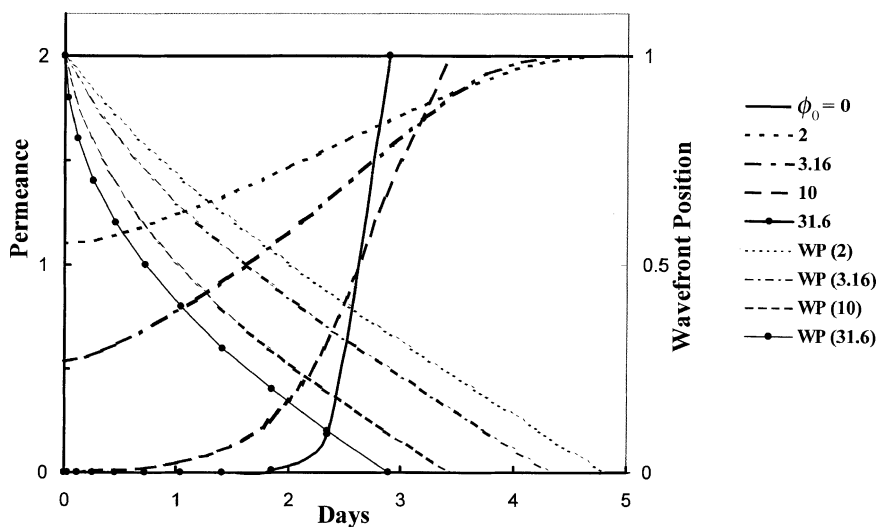

FIGURE 8 Normalized permeance of R-film with propagating reaction wavefront.
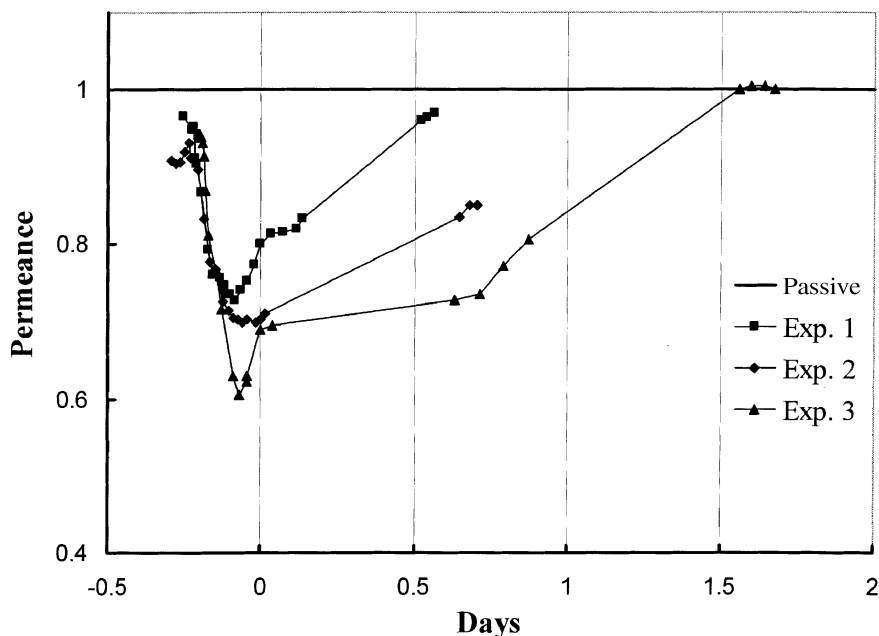
FIGURE 9 Experimental permeance data for R-film.

exhaustion time dependence on the reaction rate seen in Figure 9 is well reproduced by SG model in Figure 8 whereas the YNC model predictions for t_{LE} are independent of the reaction rate.

SUMMARY

The physical meaning of the results presented in Part II is that the scavenger capacity will be quickly exhausted in the areas exposed to high solute influx from the environment and the package contents, if the scavenging reaction rate is high as demonstrated by the result in Eq. 16.1 for the exhaustion time. When the reaction rate is low the barrier performance gain is negligible. Thus, the logical suggestion is to eliminate the permeant from the package headspace and to insulate the reactive layer from the environmental permeant load by a passive barrier layer in order to reduce the permeant concentration seen by the scavenger. That would extend the useful life of the scavenger by slowing down its consumption, or in film permeation terms: that would increase the exhaustion time before steady state permeation pattern is established.

Part III will formulate the transient solute ingress model, derive the approximate steady state lag time for non-catalytic reactive monolayer, discuss experimental methods of determining scavenging reaction rates and present comparative analysis of transient barrier performance of reactive barriers as a function of scavenger reactivity, matrix polymer properties and boundary conditions.

REFERENCES

[1] Solovyov, S. E. and Goldman, A. Y. Theory of Transient Permeation Through Reactive Barrier Films I. Steady State Theory for Homogeneous Passive and Reactive Media (this issue).

[2] Crank, J. (1975). *The Mathematics of Diffusion*, 2nd ed. (Clarendon Press, Oxford).

[3] Yang, C. Nuxoll, E. E., and Cussler, E. L. (2001). *AIChE J.* **47**(2), 295.

[4] Daynes, H. (1920). *Proc. Roy. Soc.* **A97**(685), 286.

[5] Barrer, R.M. (1951). *Diffusion In and Through Solids*. (Cambridge University Press, Cambridge).

[6] Siegel, R.A. (1991). *J. Phys. Chem.* **95**, 2556.

[7] Leypolt, J.K. and Gough, D.A. (1979). *J. Phys. Chem.* **84**, 1058.

[8] Cossler, E.L. and Yang, C. (2000). *TAPPI J.* **83**, 106.